ACS Photonics

Article

pubs.acs.org/journal/apchd5

Enhanced Photoresponsivity of a Germanium Single-Nanowire Photodetector Confined within a Superwavelength Metallic Slit

Yaohui Zhan,[†,‡] Xiaofeng Li,*[,†,‡] Dang Yuan Lei,[§] Shaolong Wu,[†,‡] Chinhua Wang,[†,‡] and Yao Li*[,⊥]

[†]College of Physics, Optoelectronics and Energy & Collaborative Innovation Center of Suzhou Nano Science and Technology, Soochow University, Suzhou 215006, China

[‡]Key Lab of Advanced Optical Manufacturing Technologies of Jiangsu Province & Key Lab of Modern Optical Technologies of Education Ministry of China, Soochow University, Suzhou 215006, China

[§]Department of Applied Physics, The Hong Kong Polytechnic University, Hong Kong, China

[⊥]Center for Composite Materials, Harbin Institute of Technology, Harbin 150001, China

ABSTRACT: Single nanowire photodetectors (SNPDs) have recently gained much attention due to their unique photonic and electronic properties. We design a germanium SNPD confined inside a silver slit and demonstrate that properly engineering the slit into superwavelength scale is able to dramatically enhance the SNPD photoresponsivity to transverse electric incidence. The light absorption by this rationally designed device can be over 3.7 times that of its subwavelength counterpart based on plasmonic resonance under transverse magnetic incidence. An extensive investigation on polarization dependence, field profile, photon flux distribution, and azimuthal absorption pattern in the SNPD reveals that the underlying mechanism responsible for the significant performance enhancement is the optimal light−nanowire coupling, benefiting from strong interference-directed light concentration inside the slit cavity. This work provides us new insights, beyond the mostly studied plasmonic enhancement effects, into photoresponsivity optimization of SNPDs.

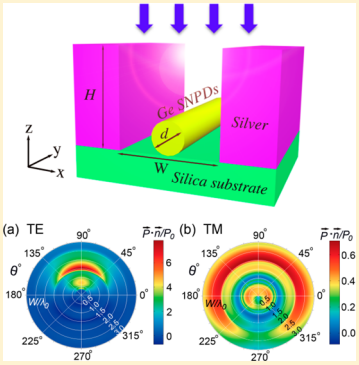

KEYWORDS: *single-nanowire photodetector, metallic slit, photodetector−light coupling, superwavelength structure, photoresponsivity*

Semiconductor nanowires are important building blocks for nanoscale optoelectronic systems due to their ease of synthesis and unique optical, thermal, mechanical, and electrical properties.[1,2] Specifically, individual semiconductor nanowires are attracting increasing interest since they can function as miniaturized photodetectors with high photoresponsivity, fast response speed, low signal-to-noise ratio (SNR), and low power consumption.[3−6] Moreover, significant shrinking of the photodetector size complies well with the development trend of electro-optical circuit integration on the nanoscale. However, an unfavorable effect arising from miniaturizing the photodetectors [e.g., single-nanowire photodetectors (SNPDs)] is the degraded photoabsorption due to less photoactive material utilized. A variety of light-trapping strategies for absorption enhancement based either on off-resonance or on-resonance schemes have therefore been developed.[7] The on-resonance mechanisms include resonant contribution by leaky modes,[8−10] surface plasmons (SPs),[11] optical Mie scattering,[12] and so on. In particular, the SP resonance is widely utilized by nanoconstructing metallic structures (embedded silver nanowires,[13,14] adhered silver nanoparticles,[15] metallic nanoparticle arrays,[16] etc.) for integration with one-dimensional semiconductor nanowires. Such metallic nanostructures can also be deemed as optical antennas that receive and reemit radiation into the nanoscale photodetection devices.[17] More recently, metallic dipole antennas are redesigned and fabricated delicately to form a subwavelength gap where an SNPD is positioned in the bottom-center of the gap. Benefiting from SP modes supported by the metallic antenna, the SNPD gains a broadband absorption enhancement of a factor of 1.7 at the target wavelength of ∼655 nm.[18] A similar concept is also used to improve the spectral response of germanium (Ge) SNPDs at a wavelength beyond the material band-edge, obtaining a high photoresponsivity across the entire telecommunication band.[19]

Although it is of no doubt that absorption enhancement can be realized by subwavelength antennas, it is solely effective under transverse-magnetic (TM) incidence since the underlying enhancement mechanism is based on SP excitations.[20,21] However, in realistic detection applications, transverse-electric (TE) and unpolarized incidences are always encountered and should be taken into account. Due to stronger coupling efficiency of the TE-polarized incidence and the Fabry-Pérot (FP) resonances supported in a slit cavity, it is natural to adjust the slit height at the wavelength scale such that the FP resonances match better with the absorption of semiconductor nanowires placed in the slit.[18] In addition, there exist alternative effective means to control and further improve the detector's photoresponsivity. For example, the metallic slit can also be configured into sub- or superwavelength scales, where

Received: November 19, 2013
Published: May 15, 2014

plasmonic absorption enhancement or improved nanowire–light coupling can be realized.

In this work, we focus on the improvement of light absorption by a slit-coupled SNPD with slit sizes comparable to the wavelength of interest. Particularly, the polarization sensitivity of the device's photoresponse is examined systematically. Compared to previous studies, two distinct observations are made: (1) the designed photodetection system shows much higher photoresponsivity under TE incidence, i.e., ~3.7 times that under TM incidence; (2) counterintuitively, a superwavelength slit works much better than its subwavelength counterpart in improving the photodetection performance. This study provides new insights into the design of chip-scale photodetectors with a substantially improved photoresponsivity.

The proposed SNPD is sketched in Figure 1, where a germanium nanowire is located inside the slit etched in a silver

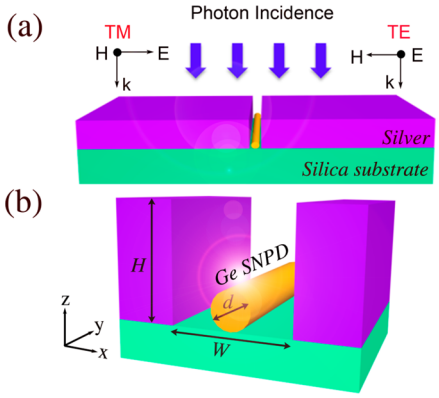

Figure 1. Sketch of a Ge SNPD located in a slit etched in a silver film: (a) global view and (b) zoom-in view.

film (slit width: W; slit height: H) supported on a silica substrate. In accordance with ref 18, the nanowire diameter and the target wavelength are 90 nm and λ_0 = 655 nm, respectively, which is due to the fact that only the fundamental mode can be sustained in such a nanowire, resulting in a single peak at the resonance wavelength. According to our simulations, H/λ_0 = 1.0 yields the best absorption performance and will be used throughout this study. The definitions of TE and TM polarizations are shown in Figure 1 in accordance with convention.[22−24] The electromagnetic response of the whole system is obtained by solving rigorously Maxwell's equations using the full-wave finite-element method.[25]

The photoresponse, characterized by the absorption efficiency Q_{abs} of the Ge SNPD, is given as a function of the ratio of slit width and the target wavelength in Figure 2. Q_{abs} is defined as the absorption cross section C_{abs} divided by the geometric cross section C_{geom}; that is, $Q_{abs} = C_{abs}/C_{geom}$. The geometric cross section is defined as the product of diameter and length of the nanowire, which can be reduced to the value of diameter in a two-dimensional model considering the ultrahigh length/diameter ratio for a typical nanowire structure. According to the polarization sensitivity shown in Figure 2, two branches can be defined with the border of line I (i.e., W/λ_0 = 0.46). On the left side of line I, the photoresponse to TM incidence is much greater than that to TE incidence ($Q_{abs} \approx 0$). This can be understood from the fact that the slit is too narrow (deep-subwavelength) to allow for transmitting any TE-polarized light; however, the TM incidence can penetrate

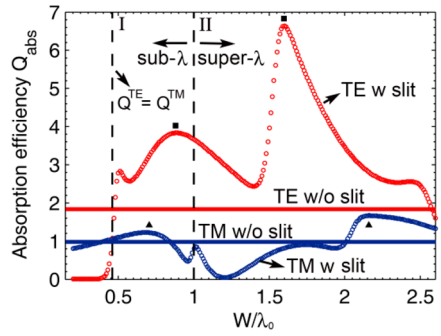

Figure 2. Absorption efficiency (Q_{abs}) spectra for TE- (red circle) and TM-polarized (blue circle) incidences as a function of normalized slit width W/λ_0. The absorption efficiencies of an isolated Ge SNPD (i.e., without (w/o) the slit) under TE (red solid line) and TM (blue solid line) incidences are given as reference.

into the slit due to the excitation of strongly localized SP modes (i.e., extraordinary optical transmission[26]). On the contrary, if $W/\lambda_0 > 0.46$, the light absorption to TE incidence is significantly improved and exhibits a much higher Q_{abs} far beyond that of TM incidence. Within the subwavelength range, the optimal widths for TE and TM incidences are $0.88\lambda_0$ and $0.68\lambda_0$ (see the square and triangle within the region between lines I and II), respectively, corresponding to enhancement factors of 2.08 and 1.25 (with respect to an isolated Ge nanowire without the presence of the silver slit). More importantly, enlarging the slit width into the superwavelength range (on the right side of line II), the enhancement factor can reach 3.61 for TE ($W = 1.6\lambda_0$), while it slight increases to 1.7 for TM ($W = 2.16\lambda_0$). Moreover, the real Q_{abs} under the superwavelength configuration can be close to 7 for TE incidence, which is more than 3.7 times that for TM incidence. This indicates that a very high photoresponsivity can indeed be obtained by using a superwavelength slit configuration for the SNPD system. Such a significant enhancement is particularly important for single-nanowire-based optoelectronic devices, including both photodetectors and solar cells.[15,18−20] Figure 2 also shows that the nanowire inside the slit can obtain much higher Q_{abs} under TE incidence than that without the slit as long as $W/\lambda_0 > 0.46$, and this cannot be achieved with TM incidence, as demonstrated by its moderate enhancement in Q_{abs}. In addition, the system can also be used to select or identify light polarization since the absorption contrast can be extremely high in some special cases, e.g., (1) $Q_{abs} \approx 0$ (for TE) as $W/\lambda_0 < 0.4$ and (2) $Q_{abs} \approx 0$ (for TM) when $W/\lambda_0 \approx 1.2$.

To reveal the physical mechanisms responsible for the absorption enhancement in the slit-coupled SNPD, the electric near-field profiles at both TE and TM incidences are shown for various slit widths in Figure 3. When the slit width is below the diffraction limit, e.g., W/λ_0 = 0.32, the TE-polarized light is completely cut off (Figure 3a), resulting in a zero photoresponse. However, the excitation of localized SP modes enables the propagation of the TM-polarized light in such a narrow slit (Figure 3f), in which a standing FP resonance is prominent.[20] Despite so, the corresponding Q_{abs} is still low compared to the stand-alone single-nanowire system (Figure 2), mainly because a significant amount of the incident photons are directly reflected by the metal surface. In Figure 3b and g, W/λ_0 is increased to 0.5, which allows the slit to capture more light at both TE and TM incidences, generating a slightly higher Q_{abs}. As Figure 2 has shown that the system response is

dx.doi.org/10.1021/ph400129t | ACS Photonics 2014, 1, 483−488

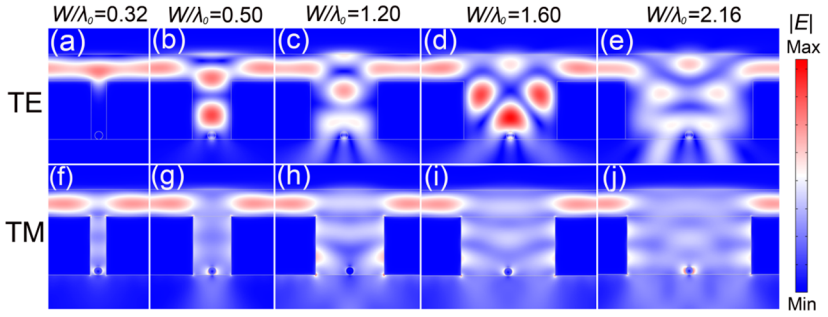

Figure 3. Normalized electric field profiles at different slit widths under TE (upper row) and TM (bottom row) incidences.

extremely sensitive to slit width, a wider slit does not certainly lead to a higher absorption due to energy redistribution. For instance, Figure 3h and i show that the light absorption by the Ge nanowire is decreased because most photon energy is confined in the silver/air interfaces due to the excitation of SP waves at TM incidence. This suggests that the Q_{abs} in SNPDs is not only determined by the coupling efficiency of the incident light into the slit but also greatly affected by the spatial distribution of the captured photon flux. Further increase of the slit width to $1.6\lambda_0$ creates strong interference in the slit under TE incidence, as confirmed in Figure 3d, where the wavefront of the normal-incident TE-polarized light is redirected by the silver slit toward the photodetector, resulting in a high SNPD−light coupling. Such an effect can be well controlled by adjusting the slit width and therefore change the phase difference between the incident and reflected light beams. At a larger slit width, e.g., $W = 2.16\lambda_0$ (Figure 3e), light confinement in the slit is too weak to generate strong light−nanowire coupling, leading to the decline of the photoresponse.

Figure 4 plots the distribution of relative power density $P(x)/P_0$ (P_0, the incident power) along the bottom line of the

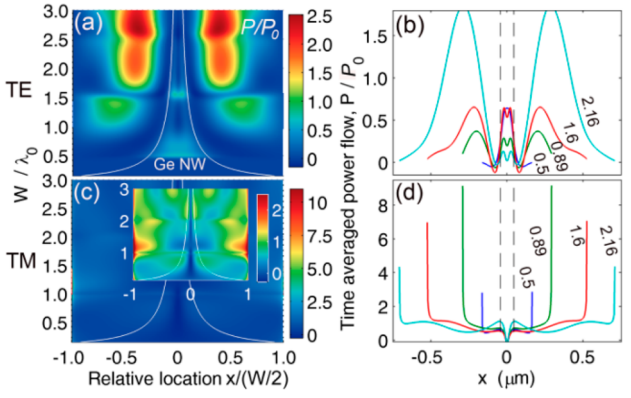

Figure 4. Contour map of normalized power flow, P/P_0, as functions of W/λ_0 and $x/(W/2)$ under (a) TE and (c) TM incidences. (b, d) Linear plots of P/P_0 versus x at various W/λ_0 values for TE and TM incidences.

slit with width varied as $0.137 \leqslant W/\lambda_0 \leqslant 3$. Considering that the slit width varies in a wide range, the relative location $x/(W/2)$ is used to construct the contour map conveniently. This way, the projection−area ratio of the Ge nanowire (with a diameter of 90 nm) will be decreased concomitantly by increasing W (see the central regions enclosed by the white lines in Figure 4a and c). In Figure 4a, under TE incidence two strong absorption regions appear in the SNPD "shadowing" area at $W/\lambda_0 = 0.5$ and 1.6, respectively, revealing that the captured light exists inside the slit within the area directly beneath the nanowire. Consequently, the light−nanowire coupling efficiency is increased, which accounts for the photoresponse peaks observed at the corresponding W/λ_0 values in Figure 2. When W/λ_0 falls between 1.0 and 1.5 or greater than 1.7, most photon energy is distributed in the region outside of the nanowire location, leading to an extremely low light−nanowire interaction. This can be further seen from Figure 4b, where the actual x position is used and multiple W/λ_0 values are taken into account. It is found that the ratio of the photon flux flowing in and out of the projection region (between dashed lines) is fairly low at $W/\lambda_0 = 0.89$ or 2.16.

Figure 4c and d show the power density distributions for the TM incidence. Different from the TE incidence, the captured photon energy is confined tightly near the slit walls ($x/(W/2) = \pm 1$) with a peak P/P_0 up to 11 (see the inset of Figure 4c) in this case. This effect is particular strong for larger slit widths well beyond the wavelength, at which excitation of a strongly localized SP mode leads to a majority of the incidence being located outside of the nanowire and hence a much lower photoresponse, as shown in Figure 2. The cross-sectional plots of the power density shown in Figure 4d further illustrate the plasmonic mode confinement in the superwavelength metallic slit, where very low energy is seen in the nanowire region. Therefore, although the SP modes can be excited in the slit by the TM-polarized light, the incident energy is mainly concentrated at the metal/air interfaces; in order to utilize the plasmonic enhancement effect to improve the SNPD photoresponse, the slit has to be narrow, which, however, leads to a relatively low absorption efficiency as shown in Figure 2 due to the unfavorable light-blocking effect.

To further elaborate the absorption characteristics of the slit-coupled Ge SNPD, the Poynting vector along the normal direction to the nanowire surface, i.e., $\vec{P}\cdot\vec{n}$, is derived to examine the azimuthal dependence of the device absorption. The radial and polar directions shown in Figure 5 represent respectively W/λ_0 and azimuthal angle θ. Figure 5a shows that,

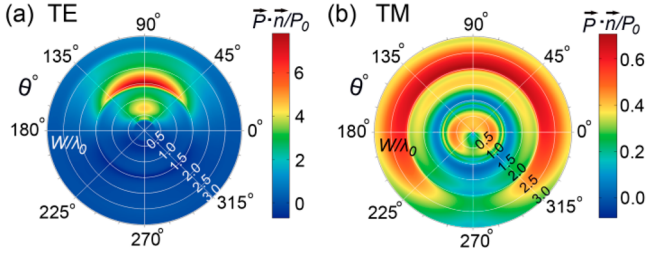

Figure 5. Azimuthal absorption patterns in the Ge SNPD under TE (a) and TM (b) incidences.

dx.doi.org/10.1021/ph400129t | ACS Photonics 2014, 1, 483−488

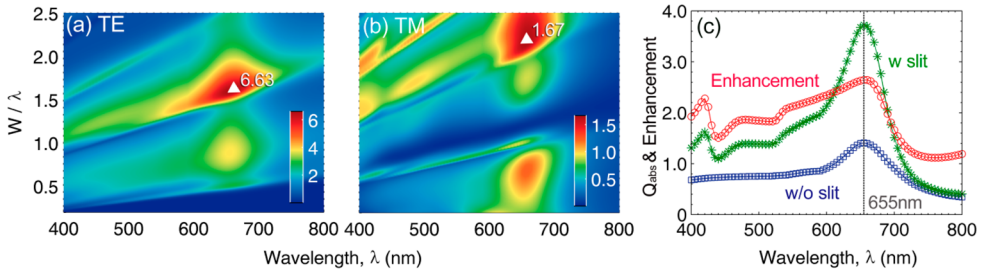

Figure 6. Contour plot of the absorption efficiency versus incident wavelength and slit width under TE (a) and TM (b) incidences. (c) Spectra of real and relative Q_{abs} for the Ge SNPD with (w) and without (w/o) the metallic slit under unpolarized incidence.

although the absorption patterns are affected dramatically by slit width, the light absorption occurs mainly within an azimuthal range from $\theta = 15°$ to $165°$ for TE incidence. For instance, with $W = 1.6\lambda_0$, the normal-incident plane wave is concentrated into a region with $45° < \theta < 135°$. This means that the properly designed silver slit functions as an efficient optical antenna, directing the TE light efficiently toward the Ge nanowire. On the other hand, the TM-polarized light can be trapped around the nanowire from nearly all azimuthal directions. As shown in Figure 5b, the shady face ($180° < \theta < 360°$) of the nanowire also contributes significantly to the overall light absorption, especially as W/λ_0 is around 0.5 or 2.16. However, the absorption efficiency of the Ge nanowire over all azimuthal directions is much lower compared to the TE case, resulting in a lower overall photoresponse.

Next, the spectral response of the slit-coupled Ge SNPD is investigated as a function of slit width. As shown in Figure 6a and b, Q_{abs} is strongly dependent not only on W but also on λ, reflecting complicated interaction behaviors between the incident light and the metal slit. In general, for either TE or TM incidence, the resonance wavelength red-shifts as the slit width increases; in the meantime, more than two absorption peaks appear at different slit widths in the wavelength range of $\lambda < 700$ nm. The maximal Q_{abs} values of the Ge SNPD are 6.63 and 1.67 for TE and TM incidences, respectively, at the same target wavelength of 655 nm, corresponding to the intrinsic resonance frequency of the Ge nanowire (see blue line in Figure 6c). Then, we examine the spectral photoresponse of the optimally designed Ge SNPD with a silver slit of $W = 1.6\lambda_0$ under unpolarized illumination. In our calculations, the unpolarized illumination is acquired by directly averaging the TE- and TM-polarized light. As shown in Figure 6c, the peak Q_{abs} of the isolated nanowire is around 1.2, while the introduction of an optimized metallic slit can significantly enhance the photoresponse, and, most importantly, such integration does not alter the resonance position in the spectrum, enabling many flexibilities in design and control of photodetection systems. A direct comparison indicates that, with the aid of the slit, the absorption efficiency at the target wavelength can be increased up to 3.72, resulting in an enhancement factor of 2.64. In addition, the spectral contrast is further improved, which could lead to higher SNR for applications such as optical signal processing.

To understand the origin of the spectral peaks observed in Figure 6, the waveguide characteristics of a single metallic slit is explored further. According to classic electrodynamics, the field distribution in a mirror waveguide can be described as the superposition of two light waves propagating oppositely toward the $+x$ and $-x$ directions,

$$\begin{cases} E_y(x, z) = E_0(e^{ik_0\sigma_x x} + e^{-ik_0\sigma_x x})e^{ik_0\sigma_z z} \rightarrow (\text{TE}) \\ H_y(x, z) = H_0(e^{ik_0\sigma_x x} + e^{-ik_0\sigma_x x})e^{ik_0\sigma_z z} \rightarrow (\text{TM}) \end{cases} \quad (1)$$

where E_0 (H_0) is the incident electric (magnetic) amplitude, $\sigma_{x(z)}$ the effective index along the x (z) direction and k_0 the wavevector in free space. By matching the boundary conditions, i.e., $E_y = H_x \approx 0$ for TE incidence and E_x and H_x with finite values, eq 1 can be reduced to $\sigma_z(W, k_0)$, as functions of slit width and incident wavevector,

$$\begin{cases} \dfrac{\sqrt{1-\sigma_z^2} + \sqrt{\varepsilon-\sigma_z^2}}{\sqrt{1-\sigma_z^2} - \sqrt{\varepsilon-\sigma_z^2}} = e^{ik_0W\sqrt{1-\sigma_z^2}} \rightarrow (\text{TE}) \\ \dfrac{\varepsilon\sqrt{1-\sigma_z^2} + \sqrt{\varepsilon-\sigma_z^2}}{\varepsilon\sqrt{1-\sigma_z^2} - \sqrt{\varepsilon-\sigma_z^2}} = e^{ik_0W\sqrt{1-\sigma_z^2}} \rightarrow (\text{TM}) \end{cases} \quad (2)$$

where $\varepsilon = \varepsilon(k_0)$ is the dielectric function of the metal. Once the incident wavelength and slit width are given, a unique solution of complex σ_z can be found numerically by solving eq 2.When $\text{Im}(\sigma_z) \approx 0$, guide modes are supported in the slit waveguide. Interestingly, it can be seen from Figure 7 that the bands of slit width corresponding to the appearance of guide modes are discrete, extremely narrow, and periodic-like to some extent. In addition, these bands seem to appear alternately along the W/λ_0 axis at different positions for TE and TM incidences and hence have few overlapping regions for the two cases. Despite so, as shown in Figure 7 (gray line), the metallic slit with $W = 1.6\lambda_0$ supports guided modes for both TE and TM incidences. These guided modes play a key role in improving the absorption efficiency of the Ge SNPD. For TE illumination, $\lambda_0 = 2W$ is the upper cutoff wavelength for the waveguide. Therefore, when $\lambda_0 > 2W$ (i.e., $W/\lambda_0 < 0.5$), the incident light is blocked off by the slit characterized by large $\text{Im}(\sigma_z)$ values as shown in Figure 7a, resulting in a dramatic decrease in the absorption of Ge SNPD as seen from Figure 2.

Finally, considering the feasibility of experimental implementation, the influence of the lateral offset of the Ge nanowire from the slit center in x direction (noted as Pos) on the azimuthal absorption is investigated. Without loss of generality, the offset direction is defined to be toward the positive x axis. As seen in Figure 8a, for TE incidence, the azimuthal photoresponse is bilaterally symmetric; however, as the offset is increased, the angle at which the absorption efficiency is maximum rotates anticlockwise because the nanowire becomes more and more distant from the convergence location of the

dx.doi.org/10.1021/ph400129t | ACS Photonics 2014, 1, 483−488

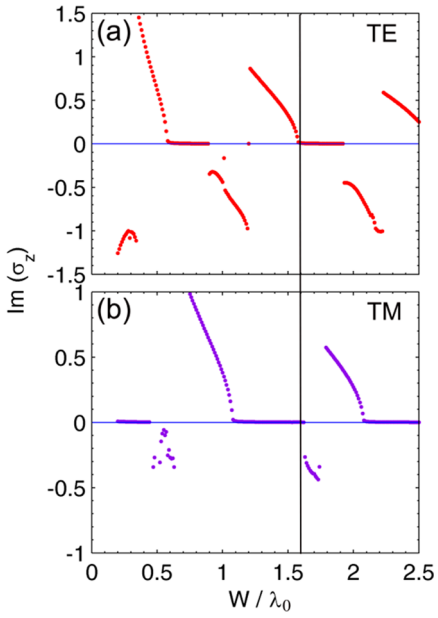

Figure 7. Mode analysis in the metallic slit under TE (a) and TM (b) incidences. The data points with $\mathrm{Im}(\sigma_z) \approx 0$ correspond to the guide modes, and the gray line indicates $W/\lambda_0 = 1.6$.

light energy. Different from the case of TE incidence, the optimum angle rotates clockwise as the nanowire approaches the slit wall as shown in Figure 8b for TM incidence. Figure 8c shows the absorption efficiency as a function of the offset at normal incidence for TE, TM, and unpolarized incidences, which further elaborate the observations made above.

In conclusion, significant enhancement in the photoresponsivity of a germanium single-nanowire photodetector has been achieved by placing it inside a superwavelength silver slit. The observed improvement shows strong dependence on the incident polarization, the slit width, and the azimuthal angle, which all are clearly revealed by the near-field profiles and the absorbed power distributions. Our results indicate that, instead of using the plasmonic enhancement mechanism in subwavelength systems, superwavelength structures with slit dimensions bigger than the incident wavelength can provide a much higher photoresponsivity. This is realized by boosting the light−photodetector coupling strength through properly steering the slit dimension, which might open a new avenue for designing compact and highly sensitive photodetectors.

AUTHOR INFORMATION

Corresponding Authors

*E-mail: xfli@suda.edu.cn (X. Li).
*E-mail: yaoli@hit.edu.cn (Y. Li).

Notes

The authors declare no competing financial interest.

ACKNOWLEDGMENTS

X.L. thanks the funding support by the National Natural Science Foundation of China (No. 91233119, No. 61204066), the "Thousand Young Talents Program" of China, Ph.D. Programs Foundation of Ministry of Education of China (20133201110021), and Priority Academic Program Development (PAPD) of Jiangsu Higher Education Institutions. Y.Z. thanks Jiangsu Planned Projects for Postdoctoral Research Funds (No. 1302100B). Y.L. thanks the National Natural Science Foundation of China (No. 51010005). D.Y.L. acknowledges grants 1-ZVAL and 1-ZVAW administrated by Hong Kong Polytechnic University.

REFERENCES

(1) Kind, H.; Yan, H.; Messer, B.; Law, M.; Yang, P. Nanowire ultraviolet photodetectors and optical switches. *Adv. Mater.* **2002**, *14*, 158−160.

(2) Logeeswaran, V. J.; Oh, H.; Nayak, A. P.; Katzenmeyer, A. M.; Gilchrist, K. H.; Grego, S.; Kobayashi, N. P.; Wang, S.-Y.; Talin, A. A.; Dhar, N. K.; Islam, M. S. A perspective on nanowire photodetectors: current status, future challenges, and opportunities. *IEEE J. Sel. Top. Quantum Electron.* **2011**, *17*, 1002−1032.

(3) Ahn, Y. H.; Park, J. Efficient visible light detection using individual germanium nanowire field effect transistors. *Appl. Phys. Lett.* **2007**, *91*, 162102.

(4) Wu, P.; Dai, Y.; Ye, Y.; Yin, Y.; Dai, L. Fast-speed and high-gain photodetectors of individual single crystalline Zn_3P_2 nanowires. *J. Mater. Chem.* **2011**, *21*, 2563−2567.

(5) Kelzenberg, M. D.; Turner-Evans, D. B.; Kayes, B. M.; Filler, M. A.; Putnam, M. C.; Lewis, N. S.; Atwater, H. A. Photovoltaic measurements in single-nanowire silicon solar cells. *Nano Lett.* **2008**, *8*, 710−714.

(6) Cao, L.; Park, J.-S.; Fan, P.; Clemens, B.; Brongersma, M. L. Resonant germanium nanoantenna photodetectors. *Nano Lett.* **2010**, *10*, 1229−1233.

(7) Liu, W. F.; Oh, J. I.; Shen, W. Z. Light trapping in single coaxial nanowires for photovoltaic applications. *IEEE Electron Device Lett.* **2011**, *32*, 45−47.

(8) Cao, L.; White, J. S.; Park, J.-S.; Schuller, J. A.; Clemens, B. M.; Brongersma, M. L. Engineering light absorption in semiconductor nanowire devices. *Nat. Mater.* **2009**, *8*, 643−647.

(9) Li, X.; Zhan, Y. Enhanced external quantum efficiency in rectangular single nanowire solar cells. *Appl. Phys. Lett.* **2013**, *102*, 021101.

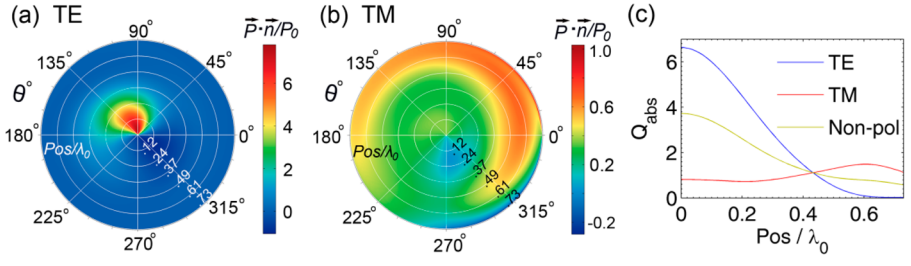

Figure 8. Azimuthal absorption pattern in the Ge SNPD as a function of the offset distance from the center under TE (a) and TM (b) incidences. (c) Absorption efficiency versus the offset distance in the unit of target wavelength at normal incidence (90°) for TE, TM, and unpolarized incidences.

(10) Zhan, Y.; Li, X.; Li, Y. Numerical simulation of light-trapping and photoelectric conversion in single nanowire solar cells. *IEEE J. Sel. Top. Quantum Electron.* **2013**, *19*, 4000208.
(11) Schuller, J. A.; Barnard, E. S.; Cai, W.; Jun, Y. C.; White, J. S.; Brongersma, M. L. Plasmonics for extreme light concentration and manipulation. *Nat. Mater.* **2010**, *9*, 193−204.
(12) Grandidier, J.; Callahan, D. M.; Munday, J. N.; Atwater, H. A. Light absorption enhancement in thin-film solar cells using whispering gallery modes in dielectric nanospheres. *Adv. Mater.* **2011**, *23*, 1272−1276.
(13) Zhan, Y.; Zhao, J.; Zhou, C.; Alemayehu, M.; Li, Y. Enhanced photon absorption of single nanowire a-Si solar cells modulated by silver core. *Opt. Express* **2012**, *20*, 11506−11516.
(14) Mann, S. A.; Garnett, E. C. Extreme light absorption in thin semiconductor films wrapped around metal nanowires. *Nano Lett.* **2013**, *13*, 3173−3178.
(15) Brittman, S.; Gao, H.; Garnett, E. C.; Yang, P. Absorption of light in a single-nanowire silicon solar cell decorated with an octahedral silver nanocrystal. *Nano Lett.* **2011**, *11*, 5189−5195.
(16) Colombo, C.; Krogstrup, P.; Nygård, J.; Brongersma, M. L.; Morral, A. F. Engineering light absorption in single-nanowire solar cells with metal nanoparticles. *New J. Phys.* **2011**, *13*, 123026.
(17) Tang, L.; Kocabas, S. E.; Latif, S.; Okyay, A. K.; Ly-Gagnon, D.-S.; Saraswat, K. C.; Miller, D. A. B. Nanometre-scale germanium photodetector enhanced by a near-infrared dipole antenna. *Nat. Photonics* **2008**, *2*, 226−229.
(18) Fan, P.; Huang, K. C. Y.; Cao, L.; Brongersma, M. L. Redesigning photodetector electrodes as an optical antenna. *Nano Lett.* **2013**, *13*, 392−396.
(19) Balram, K. C.; Audet, R. M.; Miller, D. A. B. Nanoscale resonant-cavity-enhanced germanium photodetectors with lithographically defined spectral response for improved performance at telecommunications wavelengths. *Opt. Express* **2013**, *21*, 10228−10233.
(20) Yu, Y.; Ferry, V. E.; Alivisatos, A. P.; Cao, L. Dielectric core−shell optical antennas for strong solar absorption enhancement. *Nano Lett.* **2012**, *12*, 3674−3681.
(21) Zhou, L.; Yu, X.; Zhu, J. Metal-core/semiconductor-shell nanocones for broadband solar absorption enhancement. *Nano Lett.* **2014**, *14*, 1093−1098.
(22) White, J. S.; Veronis, G.; Yu, Z.; Barnard, E. S.; Chandran, A.; Fan, S.; Brongersma, M. L. Extraordinary optical absorption through subwavelength slits. *Opt. Lett.* **2009**, *34*, 686−688.
(23) Gorkunov, M.; Podivilov, E.; Sturman, B. Transmission and scattering properties of subwavelength slits in metals. *Phys. Rev. B* **2011**, *83*, 035414.
(24) Guillaumée, M.; Nikitin, A. Y.; Klein, M. J. K.; Dunbar, L. A.; Spassov, V.; Eckert, R.; Martín-Moreno, L.; García-Vidal, F. J.; Stanley, R. P. Observation of enhanced transmission for s-polarized light through a subwavelength slit. *Opt. Express* **2010**, *18*, 9722−9727.
(25) http://www.comsol.com/.
(26) Ebbesen, T. W.; Lezec, H. J.; Ghaemi, H. F.; Thio, T.; Wolff, P. A. Extraordinary optical transmission through sub-wavelength hole arrays. *Nature* **1998**, *391*, 667−669.